Contributions of Individual Nucleotides to Tertiary Binding of Substrate by a *Pneumocystis carinii* Group I Intron†

Matthew D. Disney,‡ Sergei M. Gryaznov,§ and Douglas H. Turner*,‡

Department of Chemistry, University of Rochester, Rochester, New York 14627-0216 and Geron Corporation, 230 Constitution Drive, Menlo Park, California 94025

Received June 13, 2000; Revised Manuscript Received September 12, 2000

ABSTRACT: *Pneumocystis carinii* is a mammalian pathogen that infects and kills immunocompromised hosts such as cancer and AIDS patients. The LSU rRNA precursor of *P. carinii* contains a conserved group I intron that is an attractive drug target because humans do not contain group I introns. The oligonucleotide r(AUGACU), whose sequence mimics the 3′-end of the 5′-exon, binds to a ribozyme derived from the intron with a K_d of 5.2 nM, which is 61000-fold tighter than expected from base-pairing alone [Testa, S. M., Haidaris, G. C., Gigliotti, F., and Turner, D. H. (1997) *Biochemistry 36*, 9379−9385]. Thus, oligonucleotide binding is enhanced by tertiary interactions. To localize interactions that give rise to this tertiary stability, binding to the ribozyme has been measured as a function of oligonucleotide length and sequence. The results indicate that 4.3 kcal/mol of tertiary stability is due to a G•U pair that forms at the intron's splice junction. Eliminating nucleotides at the 5′-end of r(AUGACU) does not affect intron binding more than expected from differences in base-pairing until r(_ _ _ACU), which binds much more tightly than expected. Adding a C at the 5′- or 3′-end that can potentially form a C−G pair with the target has little effect on binding affinity. Truncated oligonucleotides were tested for their ability to inhibit intron self-splicing via a suicide inhibition mechanism. The tetramer, r(_ _GACU), retains similar binding affinity and reactivity as the hexamer, r(AUGACU). Thus oligonucleotides as short as tetramers might serve as therapeutics that can use a suicide inhibition mechanism to inhibit self-splicing. Results with a phosphoramidate tetramer and thiophosphoramidate hexamer indicate that oligonucleotides with backbones stable to nuclease digestion retain favorable binding and reactivity properties.

Pneumocystis carinii is a pathogenic fungus that infects immunocompromised hosts such as cancer and AIDS patients. For example, complications due to *P. carinii* infections are the main cause of death in AIDS patients (*1*). Treatments for *P. carinii* and other fungi are losing their efficacy because the fungi are evolving resistance to current medications (*2*). Thus, there is a need for development of new therapeutics that treat fungal infections, especially those caused by *P. carinii*.

P. carinii and several other pathogenic fungi, such as *Candida albicans* (*3*) and *Aspergillus nidulans* (*4*) contain group I introns, but humans do not. Furthermore, group I intron self-splicing is a necessary step in the maturation of rRNA (*5*). Thus, antifungal medications designed to inhibit group I intron self-splicing would be attractive because of the potential for few side effects.

Previous research has provided the basis for rational design of hexanucleotides that bind to a *P. carinii* group I intron with high specificity. In particular, oligonucleotides such as r(AUGACU), whose sequence mimics the 3′-end of the 5′-exon, bind to a truncated form of a group I intron from the LSU rRNA precursor of mouse-derived *P. carinii* (*6*, *7*). Tertiary interactions enhance r(AUGACU) binding by 61000-fold over binding by base-pairing to a hexanucleotide that mimics the exon binding site in the intron (*7*).

A nuclease-stable N3′ → P5′ phosphoramidate hexanucleotide, dn(ATGAC)rU, binds to the truncated *P. carinii* intron with a K_d of 16 nM (*6*). This hexamer also inhibits self-splicing of the LSU rRNA precursor by a suicide inhibition mechanism in which the intron catalyses ligation of the hexamer to the precursor's 3′-exon in a manner that mimics the second step of self-splicing (*8*). If this suicide inhibition occurred in vivo, then rRNA would not mature properly and the fungi presumably would not propagate.

To provide a foundation for rational optimization of oligonucleotides that target self-splicing in *P. carinii*, this paper presents the effects of shortening and increasing the length of r(AUGACU) and of using phosphoramidate and thiophosphoramidate backbones (Figure 1). The results localize tertiary interactions to a G•U base-pair that occurs at the intron's splice junction and provide insight into the requirements for inhibition of self-splicing. Since smaller oligonucleotides are known to enter cells in higher concentrations than their larger counterparts (*9*) and are less expensive to synthesize, the design of a smaller therapeutic is potentially advantageous.

† This work was supported by NIH Grant AI45398.

* To whom correspondence should be addressed. Phone: (716) 275−3207, fax: (716) 473−6889, e-mail: Turner@chem.rochester.edu.

‡ University of Rochester.

§ Geron Corporation.

10.1021/bi001345x CCC: $19.00
Published on Web 10/24/2000

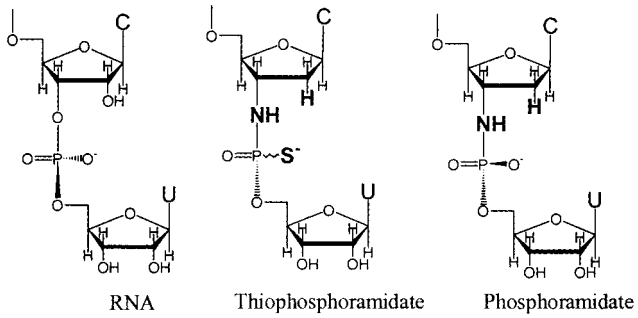

FIGURE 1: The 3′-end of oligonucleotides used in this study. Functional groups that differ from RNA are in bold. Note that in a deoxyphosphorothioate backbone (not shown), the bridging NH group of the thiophosphoramidate is replaced by an oxygen.

MATERIALS AND METHODS

Buffers. HXMg buffer is 50 mM HEPES[1] (25 mM NaHEPES), 135 mM KCl, and X mM $MgCl_2$. HEPES has a relatively low-temperature coefficient of pK_a; ΔpK_a/°C is −0.014 (*10*). The H15Mg buffer at pH 7.5 was used in all binding assays and optical melting studies; HXMg buffer at pH 6.5 was used in all precursor reactivity experiments to reduce hydrolysis at intron−exon junctions. TBE buffer is 100 mM Tris, 90 mM boric acid, and 1 mM EDTA at pH 8.4. Stop buffer contains 8 M urea, 8 mM Na_2EDTA, and 0.1× TBE buffer. The 4× RNA transcription buffer contains 40 mM Tris·HCl, 5 mM spermidine, 5 mM DTT, 40 mM $MgCl_2$, and 1 mM of each NTP at pH 7.5. The 2 M TEAA buffer was made by adding reagent-grade triethylamine to a solution containing 2 M glacial acetic acid until the pH reached 7.5.

Instruments. All HPLC chromatographs were obtained on a Hewlett-Packard Series 1100 HPLC with an attached UV/Vis detector sampling at 254 nm. Optical melting experiments were performed on a Gilford 250 UV/Vis spectrophotometer equipped with a 2527 temperature programmer. All radioactive gels were placed on chromatography paper and dried in a gel drier, and the radioactivity was quantified on a Molecular Dynamics phosphorimager with ImageQuaNT v. 4.1 software.

Synthesis and Purification of Oligonucleotides and RNA. RNA oligonucleotides were synthesized on an Applied Biosystems solid-phase synthesizer using standard protocol (*11*−*13*) from β-cyanoethyl phosphoramidites (Glen Research, Baltimore, MD) with monomer's 2′-hydroxyls protected as the *tert*-butyl-dimethylsilyl ether. They were purified and analyzed as previously described (*14*). Oligonucleotides were 5′-end-labeled with T4 kinase and [γ-^{32}P] ATP. The phosphoramidate (*15*), dn(_ _GAC)rU, and thiophosphoramidate (*16*), dns(ATGAC)rU, oligonucleotides were synthesized, deprotected, and purified as described. These oligonucleotides were further purified by TLC on a Baker Si500F plate using a 55:35:10 (v:v:v) mixture of 1-propanol, ammonia, and water as the mobile phase. The lowest running band was extracted from the plate with sterile water, and the identity of the product was confirmed by electrospray mass spectrometry on a Hewlett-Packard Series 1100 LC/MS Chemstation. The purity of each oligonucleotide was determined by reverse phase HPLC on a Supelco ABZ +Plus column (*14*). Each oligonucleotide was at least 95% pure.

The P-8/4x ribozyme was synthesized as described (*14*). The P-h precursor was internally labeled with [α-^{32}P] ATP or 3′-end-labeled with [α-^{32}P] 3′dATP as described (*17*).

Determination of K_d for Binding to the Ribozyme. The ability of oligonucleotides to bind to the group I ribozyme was determined with a competitive gel binding assay (*18*, *19*) that was adapted for this system as previously described (*6*, *7*). The method used is essentially as described (*6*, *7*) except that the ribozyme was reannealed at 55 °C for 10 min and slow cooled to 37 °C in 1× H15Mg buffer at pH 7.5. After an hour incubation at 37 °C, the bound and unbound oligonucleotides were separated at 37 °C on a 10% polyacrylamide gel containing H15Mg buffer. The fraction of r(AUGACU) bound, Θ, as a function of added competitor is given by (*14*, *18*, *19*):

$$\Theta = \frac{1}{2T_t}\left[K_t + \frac{K_t}{K_d}C_t + R_t + T_t - \sqrt{\left(K_t + \frac{K_t}{K_d}C_t + R_t + T_t\right)^2 - 4T_tR_t}\right] + A \quad (1)$$

where R_t, T_t, and C_t are the total concentrations of P-8/4x, radiolabeled r(AUGACU), and unlabeled competitor oligonucleotide, respectively; K_t is the dissociation constant for r(AUGACU) binding P-8/4x, determined from a direct gel binding assay (*7*); K_d is the dissociation constant for the competitor, and A is the fraction of r(AUGACU) apparently bound at infinite concentration of competitor. The latter corrects for a fraction of radioactivity that appears to bind covalently to the ribozyme. The competition curve is fit by nonlinear least squares for the best value of K_d, T_t, and A. All K_d values reported are the average of at least four independent measurements, and the errors given are the standard deviations in those repetitive measurements. The K_d values determined for r(_ _ _ACU), r(_ _ _ pACU), and r(AUGAC_) are considered estimates because the high oligonucleotide concentrations needed to establish a lower baseline in the curve-fit were not experimentally achievable.

Base-Pairing of 5′ Exon Mimics to a Mimic of the Intron's Internal Guide Sequence, r(GGUCAU). The free energy of base-pairing for RNA 5′-exon mimics to a mimic of the intron's internal guide sequence (IGS), r(GGUCAU), was predicted on the basis of a nearest-neighbor analysis that includes a penalty of 0.45 kcal/mol if the duplex ends in a G·U or A−U base-pair (*20*, *21*). Furthermore, the duplex stabilities account for stacking of either 5′- or 3′-dangling ends (*22*−*24*). Base-pairing for r(AUGACU**C**) was calculated by assuming the stacking of the 3′-C on the G·U pair is equal to the stacking of the 3′-C on an A−U pair (*24*).

The thermodynamics of base-pairing for the thiophosphoramidate and the phosphoramidate were determined by UV denaturation experiments. In a typical experiment, equimolar amounts of r(GGUCAU) and 5′-exon mimic were

[1] Abbreviations: dn, deoxyphosphoramidate linkages; dns, deoxythiophosphoramidate linkages; DTT, dithiothreitol; EDTA, ethylenediaminetetraacetic acid; pG, guanosine 5′-monophosphate; HEPES, *N*-[2-hydroxyethyl]piperazine-*N*′-[2-ethanesulfonic acid]; HPLC, high performance liquid chromatography; IGS, internal guide sequence; LSU, large subunit; m, methylphosphonate linkage; NTPs, ribonucleotide triphosphates; p, terminal phosphate; rRNA, ribosomal ribonucleic acid; s^2U, 2-thiouridine; s^4U, 4-thiouridine; TLC, thin-layer chromatography; Tris, tris[hydroxymethyl]aminomethane.

mixed at a concentration range of 10−600 μM. The samples were dried in vacuo and dissolved in the appropriate amount of H15Mg buffer. A temperature gradient from 0 to 60 °C was applied. The resulting absorbance versus temperature curves were fit to a two-state non-self-complementary model to extract thermodynamic parameters (*25*, *26*). Thermodynamics were calculated from both the average curve fit parameters and $1/T_M$ versus $\ln(C_T/4)$ plots. At least six different concentrations over a 60-fold range were analyzed for each sequence. The oligonucleotide r(GGUCAU) can form a self-complementary duplex that may contribute to the thermodynamics; thus, all parameters determined experimentally are considered estimates (*7*).

Trans-Splicing to Internally Labeled Precursor. All reactions were run in HXMg buffer at pH 6.5. The switch to pH 6.5 buffer was necessary to eliminate hydrolysis that occurs at the intron−3′-exon junction during the reaction and/or RNA reannealing periods. A solution containing internally labeled precursor in HXMg buffer was reannealed by heating at 55 °C for 5 min, cooled for 2 min at room temperature, and then incubated at 37 °C. Another solution containing 60 μM of 5′-exon mimic and 2 mM pG in HXMg buffer was incubated at 37 °C for 5 min and then added to an equal volume of the above precursor solution. Reactions were incubated at 37 °C for 1 h and stopped by the addition of a 2/3 volume of stop buffer. The 5′-exon−intron and intron splicing products were monitored to measure trans and cis-splicing, respectively. The 5′-exon−3′-exon and the 3′-exon products were not visible because of the low number of adenines in these products. Reaction products were separated on a 5% polyacrylamide, 8 M urea gel. The amount of radioactivity was corrected for the number of adenines in the products.

Dependence of Trans-Splicing on Oligonucleotide Concentration. A solution containing internally labeled precursor in H3Mg buffer at pH 6.5 was reannealed as described above and incubated at 37 °C. Then 3 μL of precursor in H3Mg buffer was added to a 3 μL solution of 2 mM GTP and serially diluted 5′-exon mimic in H3Mg buffer. The solution was incubated at 37 °C for 1 h and then stopped by the addition of a 2/3 volume of stop buffer. Reaction products were separated on a 5% polyacrylamide, 8 M urea gel, and the radioactivity was quantified. The data were corrected for the amount of hydrolysis that occurs at the intron−3′-exon junction by subtracting the percentage of 5′-exon−intron product formed when no oligonucleotide was present. The amount of radioactivity was corrected for the number of adenines in the products.

RESULTS

Binding of 5′ Exon Mimics to the P-8/4x Ribozyme. Dissociation constants for 5′-exon mimics binding to the P-8/4x ribozyme were determined with a competitive binding assay (*7*, *18*, *19*). Data for a typical experiment are shown in Figure 2. The results are listed in Table 1 and compared in Figure 3, which also shows the internal guide sequence that aligns the 5′-splice site in the rRNA precursor. The K_d values for binding of the 5′-truncated 5′-exon mimics r(_UGACU) and r(_ _GACU) are 4.7 and 30 nM, respectively, similar in magnitude to the previously reported K_d of 5.2 nM for r(AUGACU) (*7*). The trimer, r(_ _ _ACU), and

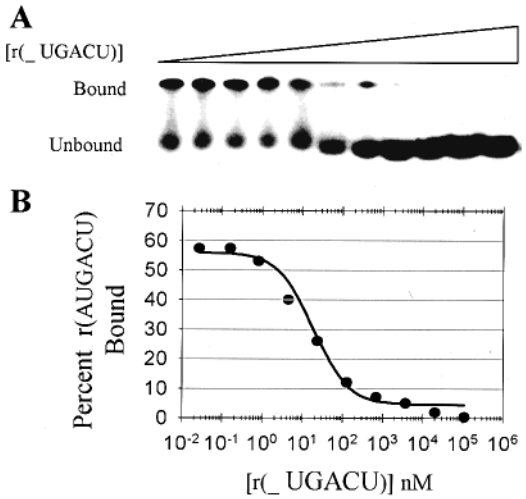

FIGURE 2: A typical competitive gel binding assay for r(_UGACU). (A) An autoradiogram of a typical experiment. (B) Plots of the data and curve-fit for r(_UGACU).

the 3′-truncated 5′-exon mimic, r(AUGAC_), bind to the ribozyme with much less favorable K_d's of 2000 and 2500 nM, respectively, roughly 500-fold weaker than r(AUGACU). Addition of a 3′-phosphate to r(AUGAC_) to yield r(AUGACp_) enhances binding by 7-fold to give a K_d of 374 nM.

The K_d's for the nuclease stable phosphoramidate, dn(_ _GAC)rU, and thiophosphoramidate, dns(ATGAC)rU, were also determined (Figure 1, Table 1). The phosphoramidate, dn(_ _GAC)rU, binds to the ribozyme with a K_d of 236 nM, which is on the order of 10-fold weaker than the K_d's of 16 and 30 nM, respectively, for dn(ATGAC)rU (*6*) and r(_ _GACU) (Table 1). The thiophosphoramidate, dns(ATGAC)rU, binds with a K_d of 122 nM, which is weaker than dn(ATGAC)rU, but stronger than the phosphorothioate, ds(ATGAC)rU [$K_d \geq 1464$ nM (*6*)]. Thus, the oligonucleotides can be protected from cellular nucleases while retaining binding affinity to the ribozyme, within a factor of roughly 10-fold.

Binding of the 5′- or 3′-extended oligonucleotides, r(**C**AUGACU) and r(AUGACU**C**), were studied because the 5′- or 3′-C has the potential of forming a base-pair to a G located immediately down- or upstream of the intron's IGS (Figure 3). The 5′- and 3′-extended oligonucleotides bind with K_d's of 2.3 and 4.5 nM, respectively, similar to the K_d of 5.2 nM for r(AUGACU). Thus addition of a 5′- or 3′-C has an insignificant effect on overall binding affinity.

Binding of the 3′-modified oligonucleotide, r(AUGAC**C**), was studied because it replaces the G·U wobble base-pair with a G−C base-pair (see Figure 3). The difference in these base-pairs is expected to have large ramifications on ribozyme binding; in *Tetrahymena thermophila*, the exocyclic amine of G in the G·U wobble pair forms tertiary interactions with the intron (*27*−*29*). When the G·U wobble pair is replaced with the G−C pair, the exocyclic amine of G is unavailable to form tertiary contacts. As expected, r(AUGAC**C**) binds more weakly to the ribozyme than r(AUGACU), with K_d of 480 versus 5.2 nM.

Base-Pairing to r(GGUCAU), a Mimic of the Intron's Internal Guide Sequence. The thermodynamics for r(AUGACU) base-pairing to r(GGUCAU) have been measured by optical melting (*7*). A nearest neighbor model (*20*,

Table 1: Ribozyme Binding K_d's, Thermodynamics of Base-Pairing, and Calculation of BETI for RNA Oligonucleotides[a]

	binding to ribozyme		binding to r(3′UACUGG5′)		tertiary interactions	
oligonucleotide	$K_{d,\,total}$ (nM)	$\Delta G^\circ_{37,\,total}$ (kcal/mole)[b]	$K_{d,B.P.}$ (mM)[b]	$\Delta G^\circ_{37,B.P.}$ (kcal/mol)	$\Delta\Delta G^\circ_{37,\,BETI}$ (kcal/mole)[c]	K_2[d] "BETI"
r(AUGACU)[e]	5.2 ± 1.0	−11.7	0.34	−4.92	−6.78	61000
r(_UGACU)	4.7 ± 1.5	−11.8	0.77	−4.42	−7.38	160000
r(_ _GACU)	30 ± 15	−10.7	1.90	−3.85	−6.85	63000
r(_ _ _ACU)[f]	≈2000	−8.1	2.4×10^3	+0.54	−8.62	1200000
r(_ _ _ _CU)	n.o.					
r(AUGAC_)[f]	≈2500	−7.9	5.00	−3.26	−4.64	2000
r(AUGAC**C**)	480 ± 25	−9.0	2.5×10^{-2}	−6.52	−2.48	53
r(AUGACp_)	374 ± 160	−9.1	5.00	−3.26	−5.84	13000
r(_ _ _pACU)[f]	≈2500	−7.9	1.7×10^3	+0.34	−8.24	680000
r(AUGACU)p	7.0 ± 0.5	−11.6	0.34	−4.92	−6.68	48000
r(**C**AUGACU)	2.3 ± 1.0	−12.3	0.21	−5.22	−7.08	104000
			(2.3×10^{-2})[g]	(−6.58)[g]	(−5.67)[g]	(11000)[g]
r(AUGACU**C**)	4.5 ± 2.1	−11.8	0.29	−5.02	−6.78	65000
			(1.3×10^{-2})[g]	(−6.93)[g]	(−4.91)[g]	(3000)[g]
dns(ATGAC)rU	122 ± 48	−9.8	0.39[h]	−4.83[h]	−4.98	3200
ds(ATGAC)rU[i]	≥1464 ± 260	−8.2	6.01	−3.15	≈−5.13	≈4100
dn(_ _GAC)rU	236 ± 80	−9.4	2.09[h]	−3.80[h]	−5.60	8840
dn(ATGAC)rU[i]	16 ± 1	−11.1	3.4×10^{-2}	−6.34	−4.72	2130

[a] Ribozyme binding K_d's were determined via competitive gel binding assays in H15Mg buffer at pH 7.5. The thermodynamics for binding by base-pairing to r(GGUCAU) were predicted on the basis of a nearest-neighbor model for increments relative to the measured binding of r(AUGACU). Underscores and bold nucleotides represent difference in sequence relative to r(AUGACU). The symbols dn, ds, and dns represent phosphoramidate, phosphorothioate, and thiophosphoramidate linkages, respectively; p represents a terminal phosphate and n.o. represents that binding to P-8/4x was not observed. [b] $\Delta G^\circ_{37,total}$ and $K_{d,BP}$ are determined from the equation $\Delta G^\circ_{37} = RT \ln(K_d)$ where R is 0.001987 kcal mol^{-1} K^{-1} and $T = 310$ K. Except for dns(ATGAC)rU and dn(_ _GAC)rU, values for $K_{d,B.P.}$ are extrapolated from the measured value for r(AUGACU). [c] The free energy of tertiary interactions is determined as the difference between the free energy of binding to the ribozyme and of base pairing. [d] K_2 is a measure of the binding enhancement by tertiary interactions (BETI) and is determined by dividing the K_d for base pairing by the K_d for ribozyme binding. [e] Ref *7*. [f] The K_d's are considered estimates because the high oligonucleotide concentrations needed to establish a lower baseline in the curve-fit were not experimentally achievable. [g] Values in parentheses are predicted if the 5′- or 3′-C forms a G−C base-pair with the intron. Values above parentheses assume only stacking of the 5′- and 3′-terminal C. [h] Thermodynamics of binding to r(GGUCAU) were measured by optical melting experiments. The ΔH° and ΔS° values from the $1/T_M$ vs $\ln(C_T)$ plots are −58.49 kcal/mol and −173.04 cal/K mol for dns(ATGAC)rU and −56.29 kcal/mol and −169.20 cal/K mol for dn(_ _GAC)rU, respectively. The ΔH° and ΔS° values from the average of curve-fits are −44.41 kcal/mol and −126.84 cal/K mol for dns(ATGAC)rU and −57.04 kcal/mol and −171.82 cal/K mol for dn(_ _GAC)rU, respectively. [i] Ref *6*.

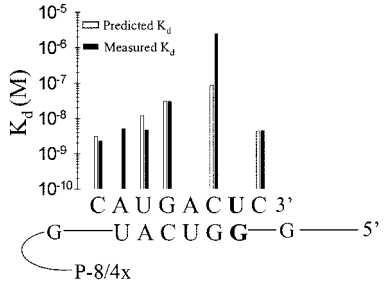

FIGURE 3: Internal guide sequence (IGS) of the ribozyme and expected pairings for oligonucleotides used in this study. Solid and open bars indicate measured and predicted K_d's, respectively, for oligonucleotides starting at the nucleotide under the bar at the 5′-end and ending with the U in the G·U pair at the 3′-end (bars at left side) or starting with the 5′-A and ending with the nucleotide under the bar at the 3′ end (bars flanking UG pair). Predicted K_d's were determined from nearest-neighbor parameters (*20*, *21*, *24*). The predicted K_d is calculated by subtracting the expected difference in the base-pairing of the oligonucleotide of interest from the $\Delta G^\circ_{37,total}$ of r(AUGACU), except for the 5′- and 3′-C's where the K_d is calculated by adding the expected free energy increment for stacking of the terminal C on its adjacent base-pair.

21, *24*) was used to extrapolate the thermodynamics for base-pairing for the other RNA 5′-exon mimics (Table 1).

The free energy increments for extending r(AUGACU) by a 5′- or 3′-C were calculated in two ways: either the 5′- or 3′-C forms a G−C base-pair with the ribozyme, or the nucleotides only stack on the adjacent base-pair (Figure 3). If the G−C base-pair forms, duplex stability is predicted to be −6.58 and −6.93 kcal/mol, respectively; if the 5′- or 3′-C's only stack on adjacent base-pairs, however, duplex stability is predicted to be −5.22 and −5.02 kcal/mol, respectively (Table 1).

The 3′-truncated oligonucleotides, r(AUGAC_) and r(AUGACp_) are predicted to base-pair similarly, with a ΔG°_{37} of −3.26 kcal/mol, because the addition of a 3′-phosphate has a negligible effect on duplex stability (*20*). The 3′-modified oligonucleotide, r(AUGAC**C**), is predicted to base-pair to the IGS, r(GGUCAU), with a free energy change of −6.52 kcal/mol at 37 °C, or 1.6 kcal/mol more tightly than r(AUGACU). Nevertheless, r(AUGAC**C**) binds to the ribozyme 100-fold more weakly than r(AUGACU) (Table 1). Evidently, tertiary interactions with r(AUGAC**C**) are particularly weak.

The free energy changes for base-pairing to r(GGUCAU) by the phosphoramidate, dn(_ _GAC)rU, and the thiophosphoramidate, dns(ATGAC)rU, were determined by optical melting experiments to be −3.80 and −4.83 kcal/mol at 37 °C, respectively. Both of the duplexes are less stable than dn(ATGAC)rU/r(GGUCAU), which has a free energy change of −6.34 kcal/mol at 37 °C (*6*). The thiophosphoramidate, however, base-pairs 1.7 kcal/mol more tightly than the equivalent phosphorothioate, ds(ATGAC)rU (Table 1).

Binding Enhancement by Tertiary Interactions (BETI). The free energy of tertiary interactions was calculated by subtracting the free energy of base-pairing, determined by either optical melting experiments or predictions, from the overall binding free-energy, determined by gel retardation (Table 1). BETI was also calculated as the ratio of the K_d's

Table 2: Free Energy Change in Tertiary Interactions ($\Delta\Delta\Delta G^\circ_{37,BETI}$) Relative to r(AUGACU) and Predicted K_d's for Binding to P-8/4x Calculated from Differences in Base-Pairing Stability Relative to r(AUGACU)

oligonucleotide	$\Delta\Delta\Delta G^\circ_{37,BETI}$ (kcal/mol)[a]	measured $K_{d,total}$ (nM)	predicted $K_{d,total}$ (nM)[b]
r(AUGACU)[c]		5.2 ± 1.0	
r(_UGACU)	−0.63	4.7 ± 1.5	12
r(_ _GACU)	0.01	30 ± 15	31
r(_ _ _ACU)	−1.79	2000	53000
r(AUGAC_)	2.14	2500	87
r(AUGAC**C**)	4.30	480 ± 25	0.34
r(AUGACp_)	0.97	374 ± 160	87
r(AUGACU)p	0.18	7.0 ± 0.5	5.2
r(**C**AUGACU)	−0.29 (1.07)[d]	2.3 ± 1.0	3.13 (0.313)[d]
r(AUGACU**C**)	0 (1.87)[d]	4.5 ± 2.1	4.4 (0.173)[d]

[a] Determined from the difference in the ΔG°_{37} of tertiary interactions between the oligonucleotide of interest and r(AUGACU). [b] The K_d's are predicted by comparing the expected duplex stabilities of the oligonucleotide with r(GGUCAU) to the duplex stability of r(AUGACU) with r(GGUCAU) and using the difference to predict the K_d for ribozyme binding on the basis of the measured ribozyme binding of r(AUGACU). [c] Ref *7*. [d] Values in parentheses are predicted if the 5′ or 3′ terminal C forms a base-pair with a G in the ribozyme. Values above the parentheses assume only stacking of the 5′ or 3′ terminal C.

for the 5′-exon mimics binding to r(GGUCAU) and to the ribozyme (*6*) (Table 1). The enhancement due to tertiary interactions quantifies the specificity of the oligonucleotide for binding the ribozyme over another target that has the same sequence as the intron's IGS.

The free energy changes for tertiary interactions are similar for r(**C**AUGACU), r(AUGACU**C**), r(AUGACU), r(_UGACU), and r(_ _GACU) (Table 1) with BETIs ranging from 60000- to 160000-fold (Table 1). The oligonucleotide trimer, r(_ _ _ ACU), however, exhibits a free energy of tertiary interactions of −8.6 kcal/mol which is almost 2 kcal/mol more favorable than that calculated for r(AUGACU). Thus, the overall binding of r(_ _ _ ACU) is 400-fold weaker than r(AUGACU), but r(_ _ _ACU) exhibits 16-fold stronger tertiary interactions.

In contrast to the mostly minor changes in the ΔG°_{37} of tertiary interactions produced by truncating r(AUGACU) from the 5′-end, removing the 3′-U reduces ΔG°_{37} of tertiary interactions by 2.1 kcal/mol (Tables 1 and 2). Evidently, the 3′-terminal U is involved in tertiary interactions that stabilize binding. Addition of a 3′-phosphate to give r(AUGACp_) results in a ΔG°_{37} of tertiary interactions that is more favorable by 1.2 kcal/mol relative to r(AUGAC_). The 3′-modified oligonucleotide, r(AUGAC**C**), exhibits a free energy of tertiary interactions that is 4.3 kcal/mol less favorable than that of r(AUGACU), thus providing further evidence that the 3′-terminal U plays an important role in tertiary interactions.

The tertiary interactions for the nuclease-stable phosphoramidate, dn(_ _GAC)rU, and the thiophosphoramidate, dns(ATGAC)rU, have ΔG°_{37} values of −5.60 and −4.98 kcal/mol, respectively. Both are similar to the value of −4.72 kcal/mol for dn(ATGAC)rU. Thus, dn(ATGAC)rU can be shortened or converted to a thiophosphoramidate without sacrificing any BETI.

Inhibition of Self-Splicing as a Function of [Mg^{2+}]. The oligonucleotides r(AUGACU), r(_UGACU), r(_ _GACU), r(_ _ _ACU), r(AUGAC**C**), dns(ATGAC)rU, and dn(_ _GAC)rU were separately incubated at a concentration of 30 μM in the presence of internally labeled precursor, 1 mM pG, and 0−15 mM Mg^{2+}. As shown in Figure 4, analysis of the splicing products relative to an experiment done in the presence of 1 mM pG and absence of oligonucleotide suggests that all of the above oligonucleotides induce formation of the 5′-exon−intron product and inhibit self-splicing at low [Mg^{2+}]. At 30 μM, the dimer and monomer, r(_ _ _ _CU) and r(_ _ _ _ _U), do not induce 5′-exon−intron product in the presence of pG (data not shown).

There are two ways a product the size of the 5′-exon−intron could be induced by the oligonucleotides. Either the oligonucleotides mimic the second step of self-splicing and are ligated to the precursor's 3′-exon or the oligonucleotides induce phosphodiester bond hydrolysis at the intron−3′-exon junction. Previous results with dn(ATGAC)rU, r(AUGACU), r(AUGACs^{2}U), r(AUGACs^{4}U), d(ATGAC)rU, and dm(ATGAC)rU, where m is a methylphosphonate backbone, indicate that the ligation, i.e., trans-splicing, mechanism predominates (*8*, *14*, *17*). To see if this is also the case for the oligonucleotides in Figure 4, their ability to trans-splice to the precursor's 3′-exon was measured using 3′-end-labeled precursor. Labeling the precursor in this manner allows direct visualization of the trans-spliced, 5′-exon mimic-3′-exon product. In each case, the oligonucleotides trans-splice to the precursor's 3′-exon (data not shown).

Comparison of the splicing profiles of r(AUGACU), r(_UGACU), r(_ _GACU), dn(_ _GAC)rU, dns(ATGAC)rU, and r(AUGAC**C**) show that these oligonucleotides induce the formation of the apparent 5′-exon−intron product similarly with regards to both Mg^{2+} dependence and efficiency. Apparently, the 2′-OH groups, O3′ → P5′ phosphodiester bonds, and the terminal G·U are not essential for this activity. The oligonucleotide r(___ACU), however, forms apparent 5′-exon−intron products with different efficiencies and Mg^{2+} dependence than the other RNA 5′-exon mimics. The efficiency of apparent trans-splicing at the optimal [Mg^{2+}] decreases from 50% for r(AUGACU), r(_UGACU), and r(__GACU) to only 30% for r(___ACU). In all of the above cases, more trans-spliced than cis-spliced product is formed until approximately 6 mM [Mg^{2+}]. Above 6 mM Mg^{2+}, the cis-spliced product dominates.

Dependence of Suicide Inhibition on Oligonucleotide Concentration. Internally labeled precursor was used to examine the dependence of trans-splicing on oligonucleotide concentration at 3 mM Mg^{2+} and 1 mM pG (Figure 5). The oligonucleotides r(AUGACU), r(_UGACU), and r(__GACU) form more trans- than cis-spliced products at concentrations greater than 300 nM. The oligonucleotide r(___ACU) forms more trans- than cis-spliced products at concentrations greater than 4000 nM. The nuclease-stable oligonucleotides, dns(ATGAC)rU and dn(__GAC)rU, form more trans- than cis-spliced product at concentrations greater than 1000 and 3000 nM, respectively.

DISCUSSION

P. carinii is a mammalian pathogen that infects and kills AIDS patients. Since *P. carinii* (*30*, *31*) and other fungal pathogens, such as *A. nidulans* (*4*) and *C. albicans* (*3*), contain group I introns but humans do not, compounds that

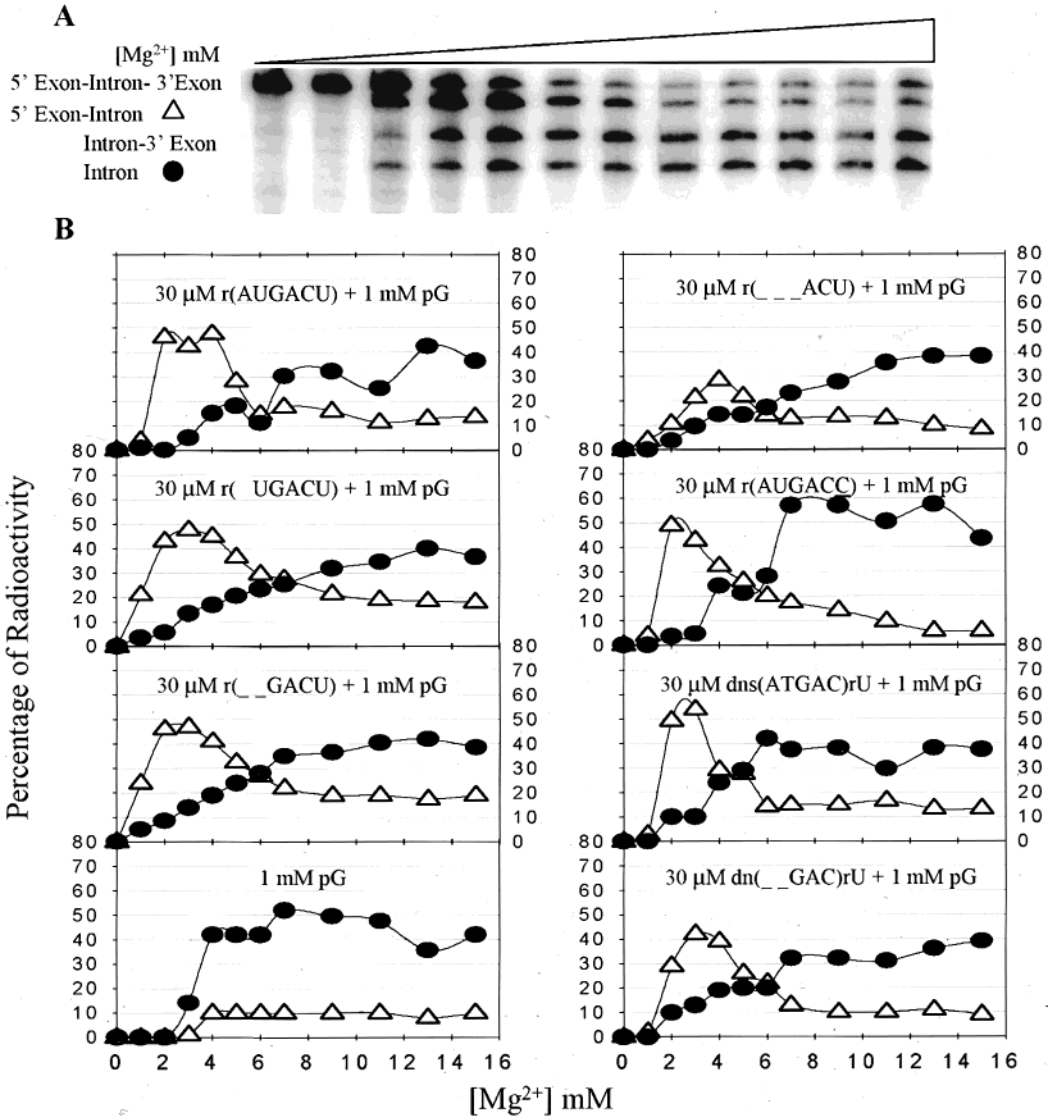

FIGURE 4: Trans- (△) and cis- (●)splicing of RNA oligonucleotides as measured with internally labeled precursor in HXMg pH 6.5 buffer. The reactions were run with 30 μM oligonucleotide and 1 mM pG, and each plot is labeled according to the reaction conditions. (A) An autoradioagram of a gel from an experiment with 30 μM r(_UGACU). (B) Plots of data for r(AUGACU), r(_UGACU), r(__GACU), r(___ACU), r(AUGAC**C**), dns(ATGAC)rU, dn(__GAC)rU, and no oligonucleotide. Each experiment was run twice, and the error is $\approx\pm$10% for each point.

target group I introns are attractive as potential therapeutics. Previously, hexanucleotides with a sequence that mimics the 3′-end of the 5′-exon have been shown to specifically bind to a ribozyme derived from the large subunit rRNA precursor of mouse-derived *P. carinii* (*6*, *7*). Binding to the ribozyme can be as much as 300000-fold tighter than to a hexanucleotide with the same sequence as the binding site in the intron (*14*). Thus, binding to ribozyme is enhanced by tertiary interactions (BETI) that are dependent on the folding of the large number of nucleotides that comprise the catalytic site.

Specific functional groups that give rise to the BETI effect have not been previously identified for the *P. carinii* ribozyme (*6*, *7*). Modification of the 5′-exon mimic (Table 1) reveals several factors that contribute to tight binding either through base-pairing or enhancements in tertiary interactions. Furthermore, the results in Figures 4 and 5 provide insight into the requirements for oligonucleotide inhibition of group I intron self-splicing. Since inhibition of intron self-splicing results in decreased organism growth (*5*), these insights into molecular recognition provide a basis for design of potential drugs for the treatment of *P. carinii* infections. The inhibitory effects correlate with the oligonucleotide's size, base composition, and backbone modifications.

Tertiary interactions have been observed for other group I introns, where the most extensively studied is the intron embedded in the rRNA of *T. thermophila* (*32*−*39*). Specific 5′-exon mimic 2′-OH groups have been implicated in forming tertiary interactions that give rise to the BETI effect in *T. thermophila* (*35*, *36*, *40*). One of these interactions is between a 5′-exon mimic 2′-OH group and an adenine in the ribozyme's J8/7 region (*41*). Tertiary interactions involving the exocyclic amine of the G in the wobble G·U pair formed at the intron's splice junction and the J4/5 region have also been elucidated for the *T. thermophila* ribozyme (*29*). Although the *P. carinii* ribozyme binds 5′-exon mimics through tertiary interactions, these interactions do not involve 5′-exon mimic 2′-OH groups (*7*). This is surprising since the J8/7 regions of *P. carinii* and *T. thermophila* ribozymes are highly homologous. To localize the tertiary interactions

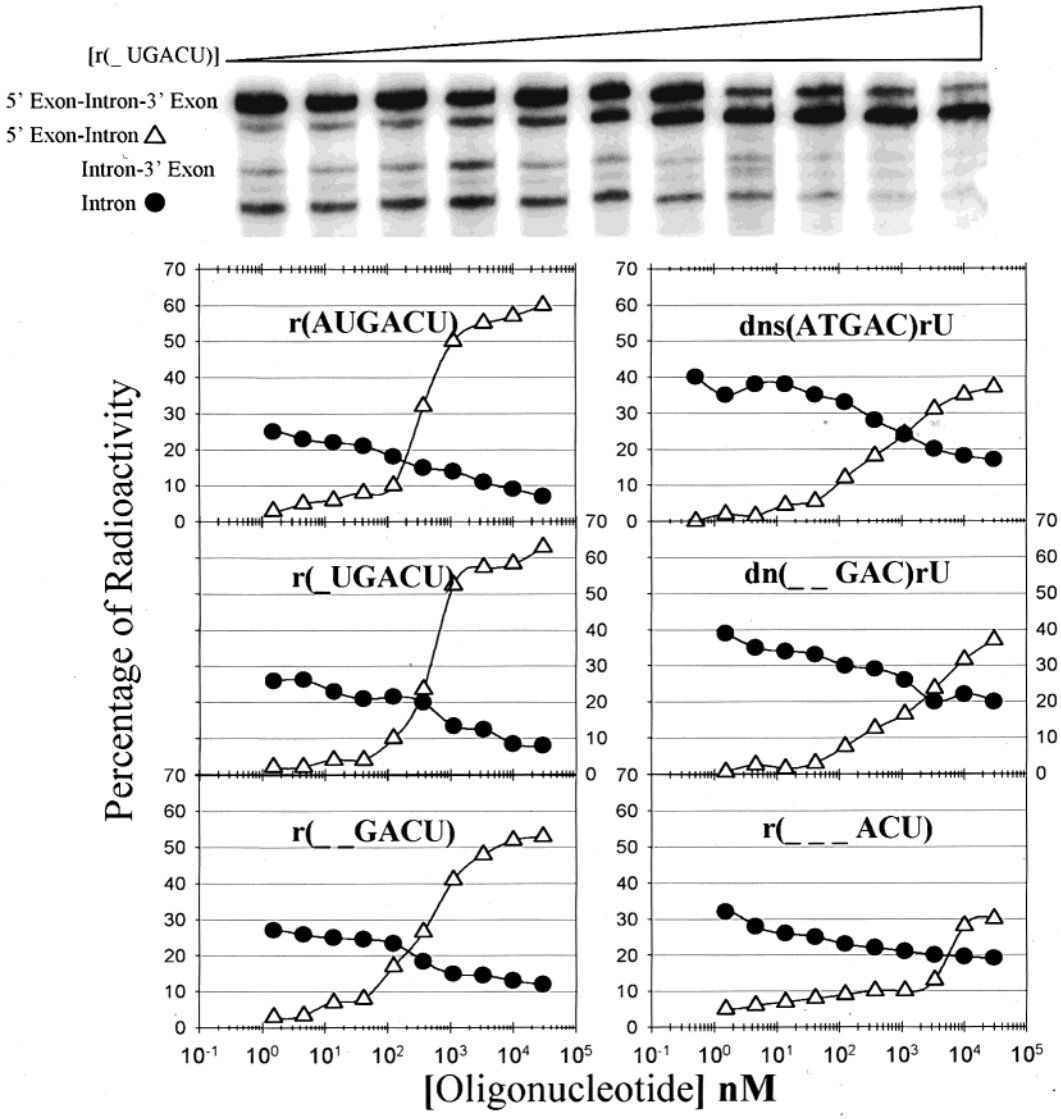

FIGURE 5: Dependence of trans- (△) and cis- (●) splicing on oligonucleotide concentration in H3Mg pH 6.5 buffer and 1 mM pG. (Top) An autoradiogram of a gel from a typical experiment with r(__GACU). (Bottom) The data obtained from those experiments. Each experiment was run twice, and the error is ≈ ± 10% for each point.

important in *P. carinii*, the energetic contributions of individual nucleotides and the terminal G·U pair to binding have been determined.

The Contributions of Individual Nucleotides to Tertiary Interactions. To determine if tertiary interactions occur to specific nucleotides, various nucleotides were removed, and the effects were quantified. Elimination of the first two 5′-nucleotides to give r(_UGACU) and r(__GACU) decreases ribozyme binding relative to r(AUGACU) in a manner expected from differences in base-pairing (Table 2 and Figure 3). Evidently, no tertiary interactions occur to these nucleotides. The observation that the BETI for dn(__GAC)rU is only 3-fold less than for dn(ATGAC)rU (Table 1) is also consistent with this interpretation. The 5′-exon mimic r(___ACU), however, has much stronger binding than expected from differences in base-pairing (Table 2). In fact, r(___ACU) exhibits the most favorable ΔG°_{37} of tertiary interactions, −8.62 kcal/mol (Table 1). This enhancement in tertiary interactions may indicate that r(___ACU) has stronger tertiary interactions than the other 5′-exon mimics and/or that r(___ACU) may alleviate one or more unfavorable tertiary interactions present with r(__GACU). In fact, the binding of both r(___pACU) and methylphosphonate deoxyoligonucleotides suggests that there may be an unfavorable tertiary interaction(s) (*14*). The binding of r(___pACU) is slightly weaker than r(__ACU), 2500 versus 2000 nM; this difference, however, in binding affinity is small, 0.2 kcal/mol, and is likely within experimental error (Table 1). Although there is only a modest difference between the binding of r(___pACU) and r(___ACU), the 5′-exon mimic d(ATGmAC)rU, where "m" is an uncharged methylphosphonate linkage, binds 2-fold tighter to the ribozyme and exhibits about 1 kcal/mol greater tertiary binding free energy than d(ATGAC)rU (*14*). Together these data suggest that there may be a small unfavorable tertiary interaction between the −3 phosphate and the ribozyme.

Binding was also measured for r(**C**AUGACU) and r(AUGACU**C**), where the 5′- or 3′-C has the potential of forming a base-pair with guanines adjacent to the intron's IGS (Figure 3). Both the 5′- and 3′-C only increase binding affinity by an amount expected if the C stacks on the adjacent A−U or G·U pairs (Tables 1 and 2). As shown in a three-dimensional model of a group I intron (*42*) (Figure 6), a nucleotide that is analogous to the G that could potentially

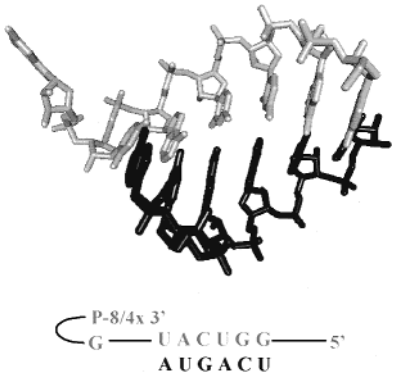

FIGURE 6: Predicted structure of the IGS·5′-exon helix for *P. carinii* based on a three-dimensional model derived from comparison of group I intron sequences (*42*). Note that the 3′-terminal G (upper left) is in a conformation that will not allow it to form a base-pair with a C added to the 5′-end of the 5′-exon.

form a base-pair with the 5′-exon mimic's 5′-C (Figure 3) is not in a conformation that can accept a base-pair. Thus, the small binding increment for adding the 5′-C provides evidence to support the three-dimensional model.

In contrast to the small effect from adding a 3′-C to r(AUGACU), removing the 3′-U to give r(AUGAC_) weakens binding dramatically to a $K_d \approx 2500$ nM (Table 1). The binding is rescued 7-fold by addition of a 3′-phosphate to give r(AUGACp_). This phosphate contributes 1.2 kcal/mol of binding energy, even though addition of 3′-phosphates has essentially no effect on duplex stability (*20*, *23*). Evidently, the phosphate contribution is mediated through tertiary interactions. Previous studies have shown that elimination of the backbone charge at this position by a phosphodiester to methylphosphonate substitution (*14*) has little effect on overall binding and tertiary interactions. Thus in the natural sequence there seems to be no tertiary interaction(s) mediated through a nonbridging oxygen that is equivalent to the oxygens of the 3′-terminal phosphate of r(AUGACp_). It is possible that r(AUGACp_) has tertiary contacts not present with r(AUGACU) or helps to preorganize the P1 helix due to steric effects. Different tertiary interactions could be mediated through the flexible, charged phosphate, which could adopt different conformations to form new tertiary interactions. In contrast, addition of a 3′-phosphate to give r(AUGACUp) has little effect on binding (Table 1). Previous kinetic measurements, however, have shown that r(CCUCU)pMe, where pMe is a methoxy phosphate, binds to the *T. thermophila* ribozyme 50-fold more weakly than r(CCUCU) (*43*). The difference between those results and ours with r(AUGACU)p may represent differences in the method of K_d determination (kinetic versus a gel binding assay), the difference between the charge on the phosphate and methoxy phosphate or a difference in how these two group I introns recognize substrate.

Examples of the effects of shortening substrate on binding to the *T. thermophila* ribozyme (*44*) and for reverse cyclization (*45*) reactions have been reported. For experiments on the ribozyme, the substrate r(CCCUCUA$_5$) was used, where the A$_5$ tail mimics the sequence downstream of the cleavage site. The experiments with the ribozyme suggest that shortening r(CCCUCUA$_5$) on the 5′-end by two nucleotides does not affect tertiary binding, but shortening the sequence by three nucleotides makes the tertiary interactions of docking less favorable by 200-fold. This contrasts with the results in Table 1, where r(___ACU) exhibits a 16-fold enhancement of tertiary interactions relative to the full-length substrate, r(AUGACU). The differences in these results could represent a difference in the tertiary interactions of the two ribozymes or could be due to the different types of substrate used in the analysis. In fact, the difference between the two types of substrate has been shown to have a surprising effect on binding. For example, adding a single 3′-A after the cleavage site to a substrate for the *T. thermophila* ribozyme makes binding less favorable by 3−40-fold (*43*, *46*), although binding is expected to be more favorable due to the dangling 3′-A (*47*). The truncated substrates studied with the *P. carinii* ribozyme do not contain nucleotides downstream of the natural cleavage site; this may produce the differences in the observed length dependence of tertiary interactions.

Base-Pairing Can Facilitate Tight Binding. The thiophosphoramidate, dns(ATGAC)rU, binds tightly due to base-pairing (Table 1). Sulfur substitution of nonbridging oxygens is often used to chemically stabilize oligonucleotides for therapeutic applications (*48*−*54*). A previous study of the phosphorothioate, ds(ATGAC)rU, however, showed that it binds the P-8/4x ribozyme with a $K_d \geq 1464$ nM (*6*). In contrast, the thiophosphoramidate binds with a K_d of 122 nM. The difference in the overall binding affinity is due to the differential base-pairing of the two oligonucleotides: for ds(ATGAC)rU, ΔG°_{37} of base-pairing is approximately −3.15 kcal/mol (*6*), but for dns(ATGAC)rU it is −4.83 kcal/mol (Table 1). Both dns(ATGAC)rU and ds(ATGAC)rU bind to the ribozyme with similar ΔG°_{37} of tertiary interactions of about −5 kcal/mol. Thus strong base-pairing can compensate for weak tertiary interactions to yield binding sufficient for potential use as a therapeutic.

The Energetic Role of the G·U Wobble Pair. The 5′-exon mimic r(AUGAC_) cannot form the G·U wobble pair at the intron's splice site. The binding of r(AUGAC_) is reduced 500-fold as compared to the binding of r(AUGACU); K_d's are 2500 and 5.2 nM, respectively. Prediction of the K_d of r(AUGAC_) relative to r(AUGACU) based on the difference in duplex stabilities suggests that the decrease in binding affinity is partially due to a decrease in tertiary interactions of 2.1 kcal/mol (Table 2). In the *T. thermophila* ribozyme, the exocyclic amine of G in the G·U pair that forms at the intron's splice junction is involved in tertiary interactions to the intron (*27*−*29*, *37*). The loss in tertiary interactions due to removing the U involved in the G·U pair in *P. carinii* may be due to the G·U wobble pair preorganizing G's exocyclic amine to form tertiary contacts. Alternatively, the U in the G·U pair may be directly involved in tertiary interactions (*17*) or both.

To further investigate the contribution of the G·U wobble pair, it was changed to a G−C pair by using the mimic r(AUGAC**C**). This mutation prevents the exocyclic amine of G and the O4 of U from forming tertiary contacts (*27*, *37*). Binding is reduced from a K_d of 5.2 nM for r(AUGACU) to 480 nM for r(AUGAC**C**) because tertiary interactions are less favorable by 4.3 kcal/mol (Table 2). The effect of replacing the G·U pair at the intron's splice site with a G−C pair in the *T. thermophila* ribozyme reduces tertiary interactions by ≈3.0 kcal/mol (*27*, *28*, *37*). Thus, the tertiary interactions of the G·U base-pair are ≈1.3 kcal/mol more

favorable in the *P. carinii* than in the *T. thermophila* ribozyme.

The large difference in the apparent contribution of the G·U base-pair to tertiary interactions in the two introns provides additional evidence that these introns bind substrate differently. It has been previously shown that the *T. thermophila* intron binds substrates with tertiary interactions that are mediated through 2′-OH groups on the substrate (*35*, *36*, *40*), whereas the *P. carinii* ribozyme does not (*7*). In contrast, both ribozymes use functional groups derived from the G·U wobble pair to form tertiary contacts, but the energetics of this interaction are different, ≈ -3.0 kcal/mol in *T. thermophila* and -4.3 kcal/mol in *P. carinii*. Interestingly, the substrate 2′-OH groups that form favorable interactions with the *T. thermophila* ribozyme contribute 1.6 kcal/mol of tertiary stability (*36*), which is close to the 1.3 kcal/mol difference observed in the tertiary free energies of the G·U wobble pair. Apparently, the stronger tertiary interactions with the G·U pair in *P. carinii* compensate for the lack of tertiary interactions with substrate 2′-OH groups.

Suicide Inhibition of Precursor Self-Splicing. Suicide inhibition is a design strategy that takes advantage of the catalytic potential of RNA (*8*). In suicide inhibition of group I intron self-splicing, an oligonucleotide with a sequence that mimics the 3′-end of the 5′-exon is ligated to the precursor's 3′-exon. This results in mis-spliced, nonfunctional RNAs. The effects of shortening the length of the suicide inhibitor were tested because smaller oligonucleotide therapeutics enter cells in higher concentrations than larger ones (*9*) and are less expensive to synthesize.

Experiments with internally labeled precursor, 30 μM oligonucleotide, and 1 mM pG suggest that shortening the 5′-exon mimic by two nucleotides has little effect on the efficiency and the Mg^{2+} dependence of suicide inhibition, as measured by the appearance of the 5′-exon−intron product (Figure 4). Shortening the 5′-exon mimic to r(___ACU), however, decreases the efficiency and slightly alters the Mg^{2+} dependence of self-splicing. Neither r(____CU) nor r(_____U) suicide inhibit at 30 μM (data not shown).

Changing the 3′-terminal base from a U to a C has little effect on suicide inhibition at 30 μM oligonucleotide concentration (Figure 4). In studies with the *T. thermophila* precursor in the absence of guanosine, exogenous oligonucleotides with the U to C mutation, e.g., r(CCCCC), also act as trans-splicing elements (*55*). In *T. thermophila*, the G·U pair is required for the first but not the second step of self-splicing (*56*); G·U facilitates the second step of self-splicing more than a G−C pair, however. On the basis of the results presented here, oligonucleotides that can form a G·U pair with the precursor are the best suicide inhibitors because the G·U pair contributes significantly to tertiary binding affinity and thus target specificity.

The nuclease-stable thiophosphoramidate, dns(ATGAC)rU, and phosphoramidate, dn(__GAC)rU, oligonucleotides also have trans-splicing activity at 30 μM. The thiophosphoramidate was tested in these studies because it retains the tight base-pairing of the phosphoramidate oligonucleotides but unlike the phosphoramidate is stable to acid (*16*) and thus has potential as an oral therapeutic.

The results in Figure 4 show that suicide inhibition only occurs at Mg^{2+} concentrations from 2 to 6 mM. Inhibition at these Mg^{2+} concentrations could indicate that the intron is not completely folded or is in a misfolded conformation that allows suicide inhibition. At higher Mg^{2+} concentrations, little inhibition is observed, possibly due to more compact intron folding rendering the IGS inaccessible. The Mg^{2+} concentrations where inhibition is observed are near physiological (*57*). This may indicate that a protein binds to the intron in vivo since binding of proteins to introns can organize the RNA for catalysis (*58*). If so, then efficacy of an oligonucleotide therapeutic targeting a group I intron may depend on the kinetics of protein and oligonucleotide binding to rRNA precursor.

The dependence of trans-splicing on oligonucleotide concentrations was measured at 3 mM Mg^{2+} and 1 mM pG (Figure 5). The results suggest that no suicide inhibition activity is lost for RNA oligonucleotides when two 5′-nucleotides are removed. Thus, a tetramer is potentially a therapeutic.

Current therapeutics used to treat fungal infections have been implicated in cell death due to inhibition of group I intron self-splicing. Specifically, the ability of pentamidine (*59*) and 5-fluorocytosine (*3*, *60*) to inhibit *C. albicans* growth has been shown to have a larger effect on strains that harbor a group I intron than strains that do not. Furthermore, both drugs have been shown to inhibit group I intron self-splicing in vitro and in vivo. Although these drugs can be used for treatment of fungal infections, they cause severe side effects (*61*, *62*). For example, 5-fluorocytosine can cause hematologic, gastrointestinal, and hepatic toxicity (*62*). The advantage of an oligonucleotide approach is that there is the potential for fewer side effects.

Implications for Therapeutic Design. The results in this paper reveal factors that affect binding of 5′-exon mimic oligonucleotides to a pharmacologically relevant group I intron. For example, formation of tertiary interactions with a G·U pair at the splice junction imparts a 100-fold increase in affinity and 1000-fold increase in specificity, when compared to an oligonucleotide that forms a G−C pair. Enhanced base-pairing can also be used to facilitate tight binding to the intron. For example, the tighter base-pairing of the thiophosphoramidate, dns(ATGAC)rU, relative to the phosphorothioate, ds(ATGAC)rU, improves the ribozyme binding K_d from 1500 to 120 nM. Oligonucleotide length can be reduced to a tetramer without sacrificing much binding affinity or reactivity. A tetramer may be a better therapeutic than a hexamer because it is cheaper to synthesize and potentially easier to get across cellular membranes (*9*). Thus, these insights provide a foundation for rational design of oligonucleotide based therapeutics with properties beneficial to cellular efficacy. It is likely that the principles and approaches established for targeting group I introns will also be applicable to targeting other RNAs.

ACKNOWLEDGMENT

We thank Professor Steve Testa (University of Kentucky) and Thom Barnes for suggesting the initial binding experiments on r(_UGACU) and Dr. Krisztina Pongracz for help with the preparation of thiophosphoramidates.

REFERENCES

1. Chaisson, R. E., Keruly, J., Richman, D. D., and Moore, R D. (1992) *Arch. Intern. Med. 152*, 2009−2013.
2. Sternberg, S. (1994) *Science 266*, 1632−1634.

3. Mercure, S., Montplaisir, S., and Lemay, G. (1993) *Nucleic Acids Res. 21*, 6020−6027.
4. Netzker, R., Kochel, H. G., Basak, N., and Kuntzel, H. (1982) *Nucleic Acids Res. 15*, 4783−4794.
5. Nikolcheva, T., and Woodson, S. A. (1997) *RNA 3*, 1016−1027.
6. Testa, S. M., Gryaznov, S. M., and Turner D. H. (1998) *Biochemistry 37*, 9379−9385.
7. Testa, S. M., Haidaris, C. G., Gigliotti, F., and Turner, D. H. (1997) *Biochemistry 36*, 15303−15314.
8. Testa, S. M., Gryaznov, S. M., and Turner, D. H. (1999) *Proc. Natl. Acad. Sci. U.S.A. 96*, 2734−2739.
9. Loke, S. L., Stein, C. A., Zhang, X. H., Mori, K., Nakanishi, M., Subbainghe, C., Cohen, J. S., and Neckers, L. M. (1989) *Proc. Natl. Acad. Sci. U.S.A. 86*, 3474−3478.
10. Good, N. E., Winget, G. D., Winter, W., Connolley, T. N., Izawa, S., and Singh, R. M. M. (1966) *Biochemistry 5*, 467−477.
11. Usman, N., Ogilvie, K. K., Jiang, M.-Y., and Cedergren, R. J. (1987) *J. Am. Chem. Soc. 109*, 7845−7854.
12. Wincott, F., DiRenzo, A., Shaffer, S., Grimm, S., Tracz, D., Workman, C., Sweedler, D., Gonzalez, C., Scaringe, S., and Usman, N. (1995) *Nucleic Acids Res. 23*, 2677−2684.
13. Stawinski, J., Stromberg, R., Thelin, M., and Westman, E. (1988) *Nucleic Acids Res. 16*, 9285−9298.
14. Disney, M. D., Testa, S. M., and Turner, D. H. (2000) *Biochemistry 39*, 6991−7000.
15. Grayznov, S. M., and Chen, J.-K. (1994) *J. Am. Chem. Soc. 116*, 3143−3144.
16. Pongracz, K., and Gryaznov, S. (1999) *Tetrahedron Lett. 40*, 7661−7664.
17. Testa, S. M., Disney, M. D., Turner, D. H., and Kierzek, R. (1999) *Biochemistry 38*, 16655−16662.
18. Lin, S., and Riggs, A. R. (1972) *J. Mol. Biol. 72*, 671−690.
19. Weeks, K. M., and Crothers, D. M. (1992) *Biochemistry 31*, 10281−10287.
20. Xia, T., SantaLucia, J., Jr., Burkard, M. E., Kierzek, R., Schroeder, S. J., Jiao, X. Q., Cox, C., and Turner, D. H. (1998) *Biochemistry 42*, 14719−14735.
21. Mathews, D. H., Sabina, J., Zuker, M., and Turner, D. H. (1999) *J. Mol. Biol. 288*, 911−940.
22. Turner, D. H., Sugimoto, N., and Freier, S. M. (1988) *Annu. Rev. Biophys. Biophys. Chem. 17*, 167−192.
23. Freier, S. M., Alkema, D., Sinclair, A., Neilson, T., and Turner, D. H. (1985) *Biochemistry 24*, 4533−4539.
24. Turner, D. H. (2000) *Nucleic Acids: Structures, Properties, and Functions* (Bloomfield, V. A., Crothers, D. M., and Tinoco, I., Jr., Eds.) Chapter 8, University Science Books, Sausalito, CA.
25. McDowell, J. A., and Turner D. H. (1996) *Biochemistry 35*, 14077−14089.
26. Longfellow, C. E., Kierzek, R., and Turner D. H. (1990) *Biochemistry 29*, 278−285.
27. Pyle, A. M., Moran, S., Strobel, S. A., Chapman, T., Turner, D. H., and Cech, T. R. (1994) *Biochemistry 33*, 13856−13863.
28. Knitt, D. S., Narlikar, G. J., and Herschlag, D. (1994) *Biochemistry 33*, 13864−13879.
29. Strobel, S. A., and Ortoleva-Donnelly, L. (1999) *Chem. Biol. 6*, 153−165.
30. Liu, Y., and Leibowitz, M. J. (1995) *Nucleic Acids Res. 23*, 1284−1290.
31. Sogin, M. L., and Edman, J. C. (1989) *Nucleic Acids Res. 17*, 5349−5359.
32. Cate, J. H., Gooding, A. R., Podell, E., Zhou, K. H., Golden, B. L., Kundrot, C. E., Cech, T. R., and Doudna, J. A. (1996) *Science 273*, 1678−1685.
33. Cate, J. H., Gooding, A. R., Podell, E., Zhou, K. H., Golden, B. L., Szewczak, A. A., Kundrot, C. E., Cech, T. R., and Doudna, J. A. (1996) *Science 273*, 1696−1699.
34. Shan, S. O., Yoshida, A., Sun, S. G., Piccirilli, J. A., and Herschlag, D. (1999) *Proc. Natl. Acad. Sci. U.S.A. 96*, 12299−12304.
35. Pyle, A. M., and Cech, T. R. (1991) *Nature 350*, 628−631.
36. Bevilacqua, P. C., and Turner, D. H. (1991) *Biochemistry 30*, 10632−10640.
37. Strobel, S. A., and Cech, T. R. (1995) *Science 267*, 675−679.
38. Strobel, S. A., and Cech, T. R. (1993) *Biochemistry 32*, 13593−13604.
39. Cech, T. R., and Golden, B. L. (1999) in *The RNA World* (Gesteland, R. F., Cech, T. R., and Atkins, J. F., Ed) 2nd ed., pp 321−349, Cold Spring Harbor Laboratory Press, Cold Spring Harbor, NY.
40. Sugimoto, N., Tomka, M., Kierzek, R., Bevilacqua, P. C., and Turner, D. H. (1989) *Nucleic Acids Res. 17*, 355−371.
41. Pyle, A. M., Murphy, F. L., and Cech, T. R. (1992) *Nature 358*, 123−128.
42. Michel, F., and Westof, E. (1990) *J. Mol. Biol. 216*, 585−610.
43. Narlikar, G. J., Gopalakrishnan, V., McConnell, T. S., Usman, N., and Herschlag, D. (1995) *Proc. Natl. Acad. Sci. U.S.A. 92*, 3668−3672.
44. Narlikar, G. J., Bartley, L. E., Khosla, M., and Herschlag, D. (1999) *Biochemistry 38*, 14192−14204.
45. Sugimoto, N., Kierzek, R., and Turner, D. H. (1988) *Biochemistry 27*, 6384−6392.
46. Bevilacqua, P. C., Li, Y., and Turner, D. H. (1994) *Biochemistry 33*, 11340−11348.
47. Freier, S. M., Kierzek, R., Caruthers, M. H., Neilson, T., and Turner, D. H. (1986) *Biochemistry 25*, 3209−3213.
48. Vaughn, J. P., Iglehart, J. D., Demirdji, S., Davis, P., Babiss, L. E., Caruthers, M. H., and Marks, J. R. (1995) *Proc. Natl. Acad. Sci. U.S.A. 92*, 8338−8342.
49. Wiesler, W. T., and Caruthers, M. H. (1996) *J. Org. Chem. 61*, 4272−4281.
50. Cummins, L., Graff, D., Beaton, G., Marshall, W. S., and Caruthers, M. H. (1996) *Biochemistry 35*, 8734−8741.
51. Lallier, T., and Bronnerfraser, M. (1993) *Science 259*, 692−695.
52. Wagner, R. W., Matteucci, M. D., Lewis, J. G., Gutierrez, A. J., Moulds, C., and Froehler, B. C. (1993) *Science 260*, 1510−1513.
53. De Clercq, E., Eckstein, F., Sternbach, H., and Morgan, T. C. (1970) *Virology 42*, 421.
54. Frey, P. A., and Sammons, R. D. (1985) *Science 228*, 541−543.
55. Inoue, T., Sullivan, F. X., and Cech, T. R. (1985) *Cell 43*, 431−437.
56. Barford, E. T., and Cech, T. R. (1989) *Mol. Cell. Biol. 9*, 3657−3666.
57. Harrison, P. M., and Hoare, R. J. (1980) in *Metals in Biochemistry*, pp 8−9, Chapman and Hall, New York.
58. Weeks, K. M., and Cech, T. R. (1995) *Cell 82*, 221−230.
59. Miletti, K. E., and Leibowitz, M. J. (2000) *Antimicrob. Agents Chemother. 44*, 958−966.
60. Mercure, S., Cousineau, L., Montplaisir, S., Belhumeur, P., and Lemay, G. (1997) *Nucleic Acids Res. 25*, 431−437.
61. Vasconcelles, M. J., Bernardo, M. V., King, C., Weller, E. A., and Antin, J. H. (2000) *Biol. Blood Marrow Transplant. 6*, 35−43.
62. Francis, P., and Walsh, T. J. (1992) *Clin. Infect. Dis. 15*, 1003−1018.

BI001345X